Computationally Efficient Predictive Direct Torque Control Strategy for PMSGs Without Weighting Factors

Mohamed Abdelrahem[a], Hisham Eldeeb[b], Christoph Hackl[c], Ralph Kennel[a], and Jose Rodriguez[d]
[a]Institute for Electrical Drive Systems and Power Electronics, Technical University of Munich (TUM), Germany, E-mail: mohamed.abdelrahem@tum.de (*corresponding author*), ralph.kennel@tum.de
[b]Research Group "Control of Renewable Energy Systems (CRES)", Munich School of Engineering, TUM, Germany, E-mail: hisham.eldeeb@tum.de
[c]Department of Electrical Engineering and Information Technology, Munich University of Applied Sciences, Germany, E-mail: christoph.hackl@hm.edu
[d]Faculty of Engineering, Universidad Andres Bello, Santiago, Chile, E-mail: jose.rodriguez@unab.cl

Abstract

This paper proposes a computationally efficient Predictive Torque Control (PTC) technique for permanent-magnet synchronous generators (PMSGs) without weighting factors. The proposed control strategy is based on computing the q-axis reference current from the demanded torque. Furthermore, the d-axis reference current is set to zero to achieve the maximum torque per ampere (MTPA) operation of the PMSG. Then, the reference voltage vector (VV) is directly computed from the reference current vector using the deadbeat principle. Finally, according to the location of this reference VV, only three evaluations of the cost function are required. The cost function includes only the error between the reference VV and the candidates ones, which eliminates the need of weighting factors. Therefore, the proposed control scheme overcomes the following drawbacks of the classical PTC: 1) High calculation burden, and 2) tuning of the weighting factors. Experimental results using a dSPACE DS1007 real-time platform and a 14.5 kW PMSG are presented to verify the feasibility of the proposed control method.

1. Introduction

Recently, the use of renewable energy generation units are increasing. In particular, wind power is considered one of the most promising technologies for electrical power generation. Variable-speed wind generators can be divided into: (i) doubly-fed induction generators (DFIGs), and (ii) permanent-magnet synchronous generators (PMSGs). The main feature of DFIGs is the utilization of a partial-scale (approx. 30% of the machine rating) back-to-back (B2B) power converter to tie the rotor windings of the DFIG with the grid [1]-[5]. However, a heavy multi-stage gear box, which requires maintenance and reduces the system reliability, is essential. Furthermore, the sensitivity to faults/voltage dips on the grid side is another drawback of the DFIGs [6], [7]. Therefore, the direct-driven PMSG with a full-scale B2B power converter is a viable alternative for variable-speed wind turbine technologies [1], [8]-[9].

The commonly adopted control schemes for PMSGs include vector control and direct torque control (DTC). Compared with the classical vector control techniques, DTC owns several features like elimination of coordinate transformation, robustness to parameter variations, and quick transient performance [10]. However, DTC schemes with hysteresis comparators suffer from the following disadvantages: large torque ripple and high sampling requirements for digital implementation.

Recently, model predictive control (MPC) strategies have been spread out across various fields including power electronics, electrical drives, and variable-speed wind generators [11], [12]. Predictive deadbeat (DB)-DTC techniques have been applied for permanent-magnet synchronous machines (PMSMs) in [13]. However, the main disadvantage of the DB-DTC strategies is their sensitivity to variations of the machine parameters. Another alternative is the continuous-control-set MPC (CCS-MPC), which considers the model of the system to predict its future behavior over a given prediction horizon. Then, the voltage vector that minimizes a certain cost function is selected. Finally, a modulation stage is used to generate the switching signals of the converter. The CCS-MPC has been utilized to control the PMSMs in [14], [15]. However, its high computational load is the main drawback. Taking into account the discrete nature of the power converters/inverters, the so called finite-control-set MPC (FCS-MPC) has been proposed. This technique (i.e. FCS-MPC) has been applied for various applications like voltage source converters and motor drive systems due to its advantages such as fast dynamic response, simple implementation, and handling of nonlinearities and constraints [11], [12]. Predictive current control, which belongs to FCS-MPC, has been applied for PMSGs in [9], [16]-[19] and Predictive Torque Control (PTC) has also been employed to control the PMSMs in [20]-[26].

Generally, in PTC schemes, the control variables are the torque and stator flux [20], [21]. However, prediction of the stator flux in the next sampling instant and calculation of the reference stator flux according to the maximum torque per ampere (MTPA) trajectory increase the complexity of the control system. Furthermore, a weighting factor is employed to penalize the stator flux magnitude error. This weighting factor has a significant impact on the control response, particularly on the harmonic current distortions. Furthermore, tuning of this weighting factor is normally realized by trail-and-error method, which is a time consuming technique. An empirical procedure to calculate the suitable weighting factors is proposed in [22]. However, this procedure lacks sufficient theoretical support. In [23], the principle of torque ripple minimization is used to compute the required weighting factor online. A fuzzy decision making strategy is proposed in [24] and a multi-objective ranking based method is presented in [25]. However, the main drawback of those methods is the required high calculation burden. To reduce the calculation load, the computation of the weighting factor is realized by a simple look up table technique in [26]. However, this method requires substantial offline calculation.

In this paper, firstly, the d-axis current of the PMSG is selected as the second control variable beside the torque. Accordingly, the MTPA operation is realized easily by setting the reference current of the d-axis to zero, which slightly reduces the calculation load. Secondly, in order to avoid using weighting factors in the cost function, the reference current of the q-axis is determined according to the demanded torque. Furthermore, the reference voltage vector (VV) is directly computed from the reference d- and q-axis currents using a deadbeat function. Thirdly, in order to reduce the computational effort, the sector where the reference VV is located is determined. Therefore, three evaluations of the cost function are only required to find the optimal VV to apply in the next sampling interval. The cost function contains the error between the reference VV and the candidates VVs. Accordingly, no weighting factors are required. The performance of the proposed control technique is validated experimentally and its response is compared with that of the conventional PTC scheme.

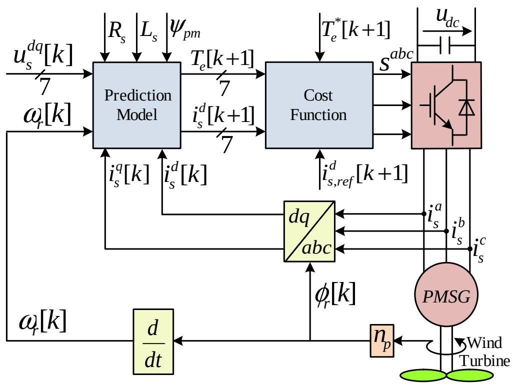

Fig. 1: Traditional PTC strategy for surface-mounted PMSGs.

2. Modeling of the PMSG

In direct-drive variable speed wind turbine systems (WTSs), the PMSG is mechanically coupled to the wind turbine via a stiff shaft (see Fig. 1). The stator windings of the PMSG are tied via a B2B power converter and a filter to the grid. The machine-side converter (MSC) is utilized to control the electromagnetic torque of the PMSG and to achieve the MTPA criteria. The continuous-time model of a three-phase surface-mounted PMSG can be written in the synchronously rotating dq-reference frame as follows [27]:

$$\left.\begin{aligned} u_s^d(t) &= R_s i_s^d(t) + \tfrac{d}{dt}\psi_s^d(t) - \omega_r \psi_s^q(t), \\ u_s^q(t) &= R_s i_s^q(t) + \tfrac{d}{dt}\psi_s^q(t) + \omega_r \psi_s^d(t), \end{aligned}\right\} \qquad (1)$$

where u_s^d, u_s^q, i_s^d, i_s^q, ψ_s^d, ψ_s^q are the d- and q-axes components of the stator voltage (in V), current (in A), and flux (in Wb) of the PMSG, respectively. R_s is the stator resistance (in Ω) of the PMSG and $\omega_r =$

$n_p\omega_m$ is the electrical angular speed of the rotor (in rad/s), where n_p is the pole pair number and ω_m is the mechanical angular speed of the rotor.

The stator flux linkage of the PMSG can be written as follows

$$\psi_s^d(t) = L_s i_s^d(t) + \psi_{pm} \quad \& \quad \psi_s^q(t) = L_s i_s^q(t). \tag{2}$$

In (2), L_s is the stator inductance (in H) of the PMSG and ψ_{pm} is the permanent-magnet flux linkage (in Wb). The dynamics of the mechanics of the (stiff) wind turbine system are given by

$$\left.\begin{aligned} \frac{d}{dt}\omega_m(t) &= \frac{1}{\Theta}(T_e(t) - T_m(t) - \nu\omega_m(t)), \\ T_e(t) &= \frac{3}{2} n_p \psi_{pm} i_s^q(t). \end{aligned}\right\} \tag{3}$$

In (3), T_e is the electro-magnetic torque (in N m) and T_m is the mechanical torque produced by the wind turbine. Θ is the overall rotor inertia (in kg/m^2) of the wind turbine and PMSG, and ν is the viscous friction coefficient (in N m s; see [28, Sec. 11.1.5]).

3. Traditional PTC scheme

The structure of the traditional PTC scheme is illustrated in Fig. 1. To design this control technique, (2) is inserted into (1) and solved for $\frac{d}{dt}\boldsymbol{i}_s^{dq}$ giving

$$\left.\begin{aligned} \frac{d}{dt} i_s^d(t) &= -\frac{R_s}{L_s} i_s^d(t) + \omega_r i_s^q(t) + \frac{1}{L_s} u_s^d(t), \\ \frac{d}{dt} i_s^q(t) &= -\frac{R_s}{L_s} i_s^q(t) - \omega_r i_s^d(t) - \frac{\omega_r}{L_s}\psi_{pm} + \frac{1}{L_s} u_s^q(t). \end{aligned}\right\} \tag{4}$$

For predicting the currents at a future sampling interval, a discrete-time model is required. Thus, the forward Euler method with a sampling time $T_s \ll 1\,\text{s}$ is applied to the time-continuous model in (4). Hence, the discrete-time model of the PMSG in the rotating dq-reference frame can be written as follows [27]

$$\left.\begin{aligned} i_s^d[k+1] &= (1 - \tfrac{T_s R_s}{L_s}) i_s^d[k] + \omega_r T_s i_s^q[k] + \tfrac{T_s}{L_s} u_s^d[k], \\ i_s^q[k+1] &= (1 - \tfrac{T_s R_s}{L_s}) i_s^q[k] - \omega_r T_s i_s^d[k] - \tfrac{\omega_r T_s}{L_s}\psi_{pm} \\ &\quad + \tfrac{T_s}{L_s} u_s^q[k]. \end{aligned}\right\} \tag{5}$$

The electro-magnetic torque can be predicted by

$$T_e[k+1] = \frac{3}{2} n_p \psi_{pm} i_s^q[k+1]. \tag{6}$$

In this work, the control variable are the torque and the d-axis current, as shown in Fig. 1. The stator voltage $\boldsymbol{u}_s^{dq}[k]$ of the PMSG can be expressed as a function of the switching state vector $\boldsymbol{s}^{abc}[k] \in$

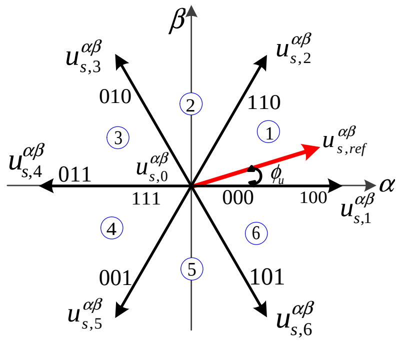

Fig. 2: Different switching combinations of 2-level voltage source converter.

$\{0,1\}^3$ of the power converter as follows [28, Chapter 14]:

$$\left.\begin{aligned} \boldsymbol{u}_s^{dq}[k] = & \underbrace{\begin{bmatrix} \cos(\phi_r) & \sin(\phi_r) \\ -\sin(\phi_r) & \cos(\phi_r) \end{bmatrix}}_{=:\boldsymbol{T}_P(\phi_r)^{-1}} \underbrace{\frac{2}{3}\begin{bmatrix} 1 & -\frac{1}{2} & -\frac{1}{2} \\ 0 & \frac{\sqrt{3}}{2} & -\frac{\sqrt{3}}{2} \end{bmatrix}}_{=:\boldsymbol{T}_C} \\ & \underbrace{\frac{1}{3} u_{dc}[k] \begin{bmatrix} 2 & -1 & -1 \\ -1 & 2 & -1 \\ -1 & -1 & 2 \end{bmatrix} \boldsymbol{s}^{abc}[k],}_{=:\boldsymbol{u}_s^{abc}[k]} \end{aligned}\right\} \tag{7}$$

where $\boldsymbol{T}_P(\phi_r)^{-1}$ and $\boldsymbol{T}_C$ are the Park and Clarke transformation matrices, respectively. u_{dc} is the DC-link voltage (in V) and $\boldsymbol{u}_s^{abc} = (u_s^a, u_s^b, u_s^c)^\top$ is the stator phase voltage vector (in V) applied to the PMSG in the abc-reference frame. $\phi_r = n_p\phi_m$ is the electrical rotor position of the PMSG (in rad). Considering all the possible combinations of the switching state vector $\boldsymbol{s}^{abc}$ as shown in Fig. 2, seven different voltage vectors can be obtained. Those seven voltage vectors can be used to predict seven future values of the current $i_s^d[k+1]$ and the electro-magnetic torque $T_e[k+1]$. Then, the following cost function

$$\begin{aligned} g = & \left|T_e^*[k+1] - T_e[k+1]\right| + \gamma\left|i_{s,ref}^d[k+1] - i_s^d[k+1]\right| \\ & + \begin{cases} 0 & \text{if} \quad T_e[k+1] \le T_{e,max}[k+1], \\ \infty & \text{if} \quad T_e[k+1] > T_{e,max}[k+1], \end{cases} \\ & + \begin{cases} 0 & \text{if} \quad \sqrt{i_s^d[k+1]^2 + i_s^q[k+1]^2} \le i_{s,max}, \\ \infty & \text{if} \quad \sqrt{i_s^d[k+1]^2 + i_s^d[k+1]^2} > i_{s,max}, \end{cases} \end{aligned} \tag{8}$$

with soft constraints is employed to select the optimal switching state vector which minimizes the cost function. This optimal switching vector is then applied at the next sampling instant. In (8), γ is a weighting factor, $T_{e,max}$ is the maximum allowable torque of the PMSG, and $i_{s,max}$ in the maximum current of the stator.

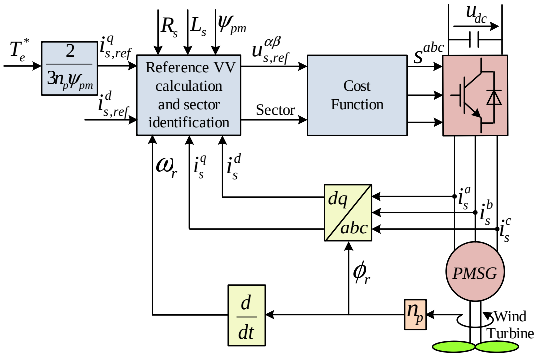

Fig. 3: Proposed PTC strategy without weighting factors for surface-mounted PMSGs.

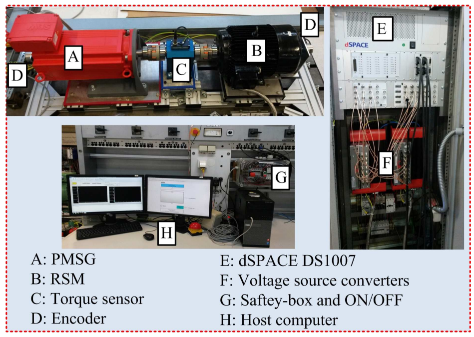

Fig. 4: Laboratory setup to validate the proposed PTC scheme for PMSGs.

The traditional PTC strategy suffers from the following disadvantages: 1) Tuning of the weighting factor γ, which is normally tuned by trial-and-error method, and 2) high calculation load.

4. Proposed PTC strategy

The proposed PTC is illustrated in Fig. 3. Firstly, the q-axis reference current $i^q_{s,ref}[k+1]$ can by computed directly from the reference electro-magnetic torque $T^*_e[k+1]$ as follows

$$i^q_{s,ref}[k+1] = \frac{2T^*_e[k+1]}{3n_p\psi_{pm}}. \tag{9}$$

Secondly, using the reference current $\boldsymbol{i}^{dq}_{s,ref}[k+1]$, the reference VV $\boldsymbol{u}^{dq}_{s,ref}[k]$ can be directly calculated using the deadbeat principle as follows

$$\left.\begin{aligned} u^d_{s,ref}[k] &= R_s i^d_s[k] + L_s \tfrac{i^d_{s,ref}[k+1]-i^d_s[k]}{T_s} \\ &\quad -\omega_r[k]L_s i^q_s[k], \\ u^q_{s,ref}[k] &= R_s i^q_s[k] + L_s \tfrac{i^q_{s,ref}[k+1]-i^q_s[k]}{T_s} \\ &\quad +\omega_r[k]L_s i^d_s[k] + \omega_r[k]\psi_{pm}. \end{aligned}\right\} \tag{10}$$

The magnitude

$$u_s[k] = \|\boldsymbol{u}^{dq}_{s,ref}[k]\| = \sqrt{u^d_{s,ref}[k]^2 + u^q_{s,ref}[k]^2}$$

of the reference voltage vector $\boldsymbol{u}^{dq}_{s,ref}[k]$ is calculated and compared with the maximally available output voltage magnitude $u_{s,max}$ of the voltage source converter which depends on the dc-link voltage u_{dc}. If the magnitude is greater than this value, the reference voltages should be adjusted as follows

$$\boldsymbol{u}^{dq}_{s,ref}[k] = \begin{cases} \boldsymbol{u}^{dq}_{s,ref}[k], & u_s[k] \le u_{s,max} \\ \frac{u_{s,max}}{u_s[k]}\boldsymbol{u}^{dq}_{s,ref}[k], & u_s[k] > u_{s,max}. \end{cases} \tag{11}$$

Tab. 1: PMSG parameters.

Name	Symbol	Value
Rated power	p_{rated}	14.5 kW
Stator line-line voltage	$u_{s,rated}$	400 V
DC-link voltage	u_{dc}	560 V
Mechanical speed	$\omega_{m,rated}$	209 rad/s
Stator resistance	R_s	0.15 Ω
Stator inductance	L_s	3.4 mH
PM flux linkage	ψ_{pm}	0.3753 Wb
Pole pairs	n_p	3

This reference VV $\boldsymbol{u}^{dq}_{s,ref}[k]$ is transformed to the stationary reference frame $\alpha\beta$ using the Park transformation. Therefore, its location can be identified as shown in Fig. 2 using its angle $\phi_u[k] = \mathrm{atan2}(u^\beta_{s,ref}[k], u^\alpha_{s,ref}[k])$. The new cost function has the form

$$g_{new} = \left|u^\alpha_{s,ref}[k] - u^\alpha_s[k]\right| + \left|u^\beta_{s,ref}[k] - u^\beta_s[k]\right|. \tag{12}$$

Based on the location of the reference VV $u^{\alpha\beta}_{s,ref}[k]$, the six sectors are defined, which are illustrated in Fig. 2. For clarification, when $\phi_u[k] \in [0, \frac{\pi}{3}]$, then the reference VV is located in sector 1 and the only reasonable candidate VVs are $u^{\alpha\beta}_{s,0}$, $u^{\alpha\beta}_{s,1}$, and $u^{\alpha\beta}_{s,2}$. Hence, (12) is evaluated for only three times to obtain the optimal VV. Moreover, there is no need to use a weighting factor in the cost function. Accordingly, the proposed PTC overcomes the disadvantages of the traditional one.

5. Description of Laboratory Setup

The proposed and traditional PTC techniques have been experimentally implemented. The setup consists of a 14.5 kW PMSG driven by a two-level voltage source converter (VSC). A 9.5 kW reluc-

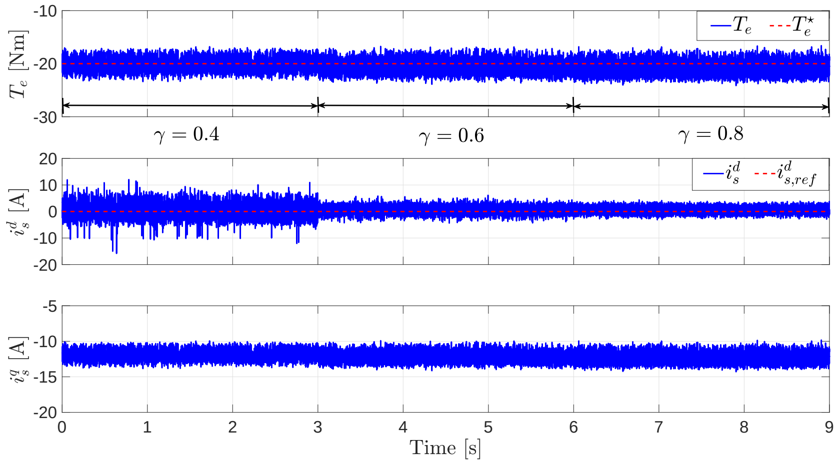

Fig. 5: Performance of the traditional PTC at different values of the weighting factor γ.

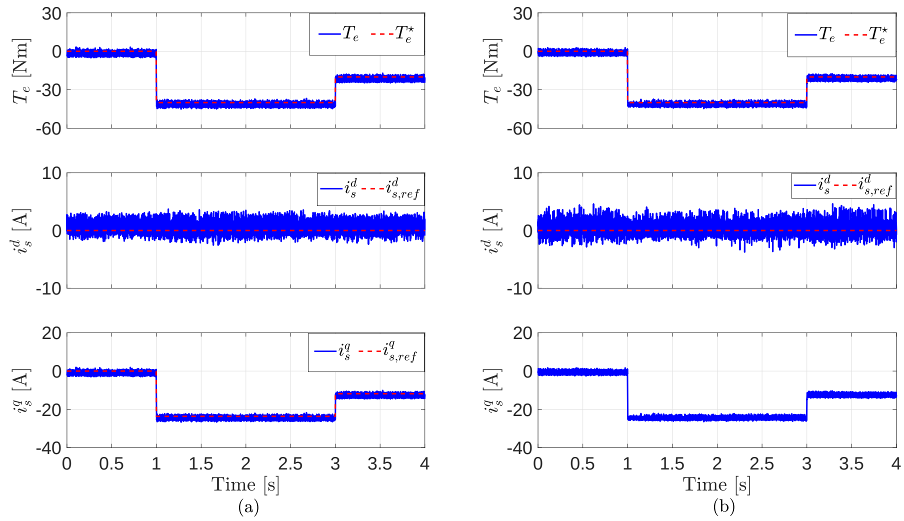

Fig. 6: Experimental results for step changes in the electro-magnetic torque T_e: (a) Proposed PTC, and (b) traditional PTC.

tance synchronous machine (RSM) driven by another two-level VSC is employed to emulate the variable-speed wind turbine dynamics and is controlled using a nonlinear current PI-based field-oriented control (FOC) technique [29]. The two machines (i.e. PMSG and RSM) are coupled through a torque sensor as illustrated in Fig. 4. The proposed and traditional PTC schemes are implemented on a dSPACE DS1007 real-time system using MATLAB/Simulink and Control Desk software. The sampling frequency is set to 11 kHz. An incremental encoder is used to measure the rotor position of the PMSG. Three current sensors and one voltage sensor are used to measure the stator currents of the PMSG and the DC-link voltage, respectively. The experimental setup is depicted in Fig. 4 and the parameters of the PMSG are listed in Table 1.

6. Experimental Results

The reference value of the electro-magnetic torque $T_e^\star$ is selected to be lower than the rated value of the RSM (i.e. $T_{RSM}^{rated} = 61$ N m) and the reference value of the d-axis current $i_{s,ref}^d$ is set to zero to achieve the MTPA condition. Fig. 5 illustrates the performance of the traditional PTC at different values of the weighting factor γ. The electro-magnetic torque is set to -20 N m by the PMSG control system and

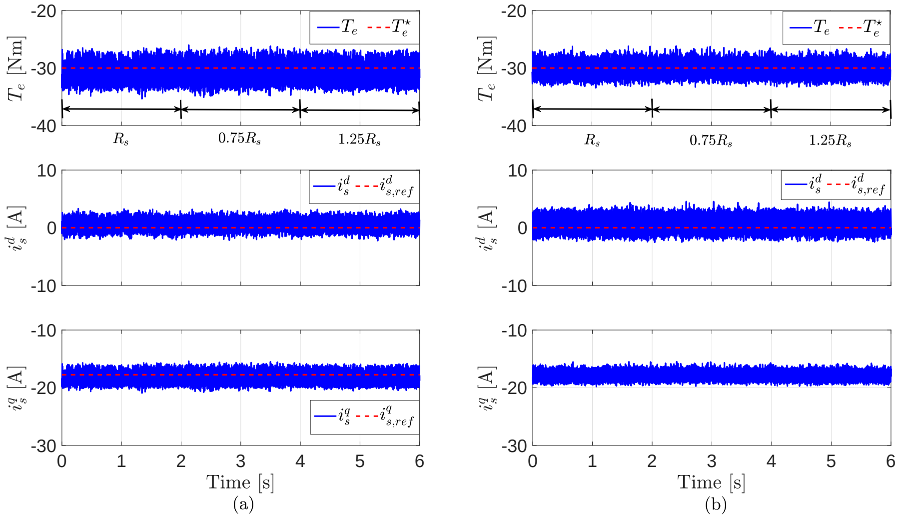

Fig. 7: Experimental results for step changes in the stator resistance R_s of the PMSG: (a) Proposed PTC, and (b) traditional PTC.

the mechanical speed of the shaft is kept constant at 100 rad/s by the RSM control technique. It is clear from this figure that the weighting factor γ is playing an important role in the ripples that appeared in the current waveform. Accordingly, the weighting factor $\gamma = 0.8$ is selected in the work.

The dynamic performance of the proposed PTC and traditional one is shown in Fig. 6. At the time instants $t = 1.0$ s and $t = 3.0$ s, step changes in the reference electro-magnetic torque $T_e^\star$ from 0 N m to -40 N m and then to -20 N m, respectively, have been applied to the PMSG control strategy. The mechanical speed of the shaft ω_m is kept constant at 80 rad/s. It can been seen from Fig. 6 that the dynamic performance of the proposed PTC is similar to that of the traditional one. However, the proposed PTC requires approximately 15 µs execution time, while the traditional PTC requires approximately 35 µs. Hence, the computational load is reduced to $\frac{15}{35} \times 100\% = 42\%$ (i.e., a reduction by 58%). Furthermore, in the proposed PTC, no effort is required for tuning of the weighting factor.

The robustness of the proposed PTC is also investigated and compared with the traditional one. In Fig. 7, the performance of the proposed PTC and traditional one for $\mp 25\%$ software step changes in the stator resistance R_s of the PMSG is illustrated. The electro-magnetic torque T_e is set to -30 N m and the mechanical speed of the shaft ω_m is kept constant at 120 rad/s. According to that figure, both control schemes (i.e. proposed and traditional PTC) show good robustness to variations of the stator resistance R_s of the PMSG.

Finally, the performance of the proposed PTC and traditional one under variations of the stator inductance L_s of the PMSG is given in Fig. 8. The electro-magnetic torque T_e is set to -25 N m and the mechanical speed of the shaft ω_m is kept constant at 90 rad/s. It can be observed that both control techniques (i.e. proposed and traditional PTC) are sensitive to mismatches in the stator inductance L_s of the PMSG. This is because predicting the torque/d-axis current and computing the reference voltage vector are highly dependent on the parameters of the machine. However, both control systems are still stable.

7. Conclusion

In this paper, a computationally efficient PTC technique without weighting factors for PMSGs is proposed. The proposed PTC strategy is based on using the d-axis current of the PMSG to be the second control variable beside the torque, which reduces (slightly) the calculation burden. Furthermore, in order to overcome the weighting factors tuning problem in the cost function, the reference current of the q-axis is computed according to the reference torque. Then, the reference VV is directly computed from the reference d- and q-axis currents using a

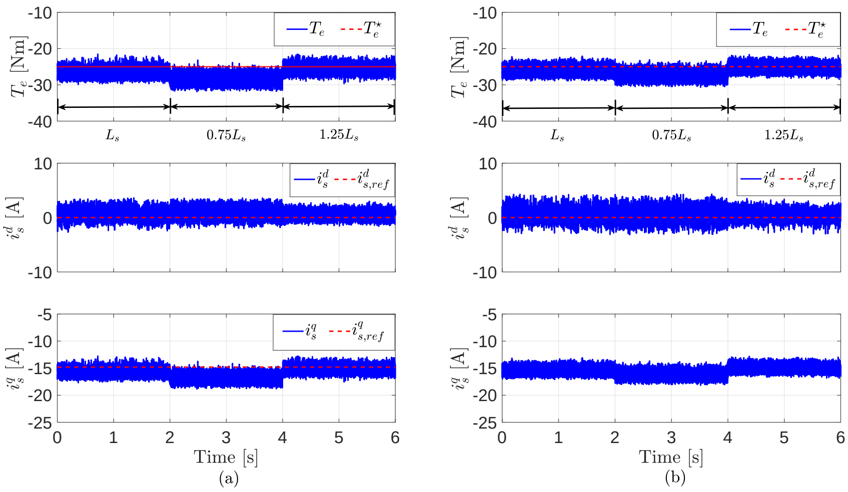

Fig. 8: Experimental results for step changes in the stator inductance L_s of the PMSG: (a) Proposed PTC, and (b) traditional PTC.

deadbeat function. Finally, in order to reduce the computational effort, the sector where the reference VV is located is determined. Therefore, three evaluations of the cost function are only required to find the optimal VV. The performance of the proposed PTC technique is experimentally investigated and compared with that of the conventional one. The results have shown that: 1) The calculation burden of the proposed PTC strategy is significantly lower that of the traditional one, 2) the dynamic/steady-state performance of the proposed PTC technique is similar to that of the traditional PTC, and 3) both the proposed and traditional PTC techniques are sensitive to variations of the machine parameters, in particular, the inductance of the stator.

8. Acknowledgment

This work is supported by the project AWESCO (H2020-ITN-642682) funded by the European Union's Horizon 2020 research and innovation programme under the Marie Sklodowska-Curie grant agreement No. 642682.

9. References

[1] M. Liserre, et. al. "Overview of Multi-MW Wind Turbines and Wind Parks", *IEEE Trans. on Industrial Electronics*, vol. 58, no. 4, pp. 1081-1095, 2011.

[2] M. Abdelrahem, R. Kennel, "Efficient Direct Model Predictive Control for Doubly-Fed Induction Generators", *Electric Power Components and Systems*, vol. 45, no. 5, pp 574-587, 2017.

[3] M. Abdelrahem, C. Hackl, and R. Kennel, "Sensorless Control of Doubly-Fed Induction Generators in Variable-Speed Wind Turbine Systems", *in Proc. of the 5^{th} International Conference on Clean Electrical Power (ICCEP)*, Taormina, pp. 406-413, 2015.

[4] M. Abdelrahem, C. Hackl, and R. Kennel, "Application of Extended Kalman Filter to Parameter Estimation of Doubly-Fed Induction Generators in Variable-Speed Wind Turbine Systems", *in Proc. of the 5^{th}ICCEP*, Taormina, pp. 226–233, 2015.

[5] M. Abdelrahem, C. Hackl, R. Kennel, "Encoderless Model Predictive Control of Doubly-Fed Induction Generators in Variable-Speed Wind Turbine Systems", *Journal of Physics: Conference Series*, vol. 753, pp. 1-10, 2016.

[6] M. Abdelrahem, M. H. Mobarak, and R. Kennel, "Model Predictive Control for Low-Voltage Ride Through Capability Enhancement of DFIGs in Variable-Speed Wind Turbine Systems", *in proceedings of IEEE 9^{th} International Conference on Electrical and Computer Engineering (ICECE 2016)*, Dhaka, pp. 70-73, 2016.

[7] M. Abdelrahem, R. Kennel, "Direct-Model Predictive Control for Fault Ride-Through Capability Enhancement of DFIG", *in proceedings of PCIM Europa*, Nuremberg, Germany, pp. 1917-1924, 2017.

[8] M. Abdelrahem, C. Hackl, R. Kennel, "Finite Position Set-Phase Locked Loop for Sensorless Control of Direct-Driven Permanent-Magnet Synchronous Generators", *IEEE Transactions on Power Electronics*, vol. 33, no. 4, pp. 3097-3105, 2018.

[9] M. Abdelrahem, R. Kennel, "Fault-Ride through

Strategy for Permanent-Magnet Synchronous Generators in Variable-Speed Wind Turbines", *Energies*, vol. 9, no. 12, pp. 1-15, 2016.

[10] G. Buja, M. Kazmierkowski, "Direct torque control of PWM inverter-fed AC motors–a survey", *IEEE Transactions on Industrial Electronics*, vol. 51, no. 4, pp. 744-757, 2004.

[11] P. Cortes, et. al., "Predictive Control in Power Electronics and Drives", *IEEE Transactions on Industrial Electronics*, vol. 55, no. 12 ,pp. 4312-4324, Dec. 2008.

[12] S. Vazquez, et. al. "Model Predictive Control for Power Converters and Drives: Advances and Trends", *IEEE Transactions on Industrial Electronics*, vol. 64, no. 2, pp. 935-947, Feb. 2017.

[13] J. Lee, et. al., "Deadbeat-Direct Torque and Flux Control of Interior Permanent Magnet Synchronous Machines With Discrete Time Stator Current and Stator Flux Linkage Observer", *IEEE Transactions on Industry Applications*, vol. 47, no. 4, pp. 1749-1758, 2011.

[14] M. Vafaie, et. al., "Minimizing Torque and Flux Ripples and Improving Dynamic Response of PMSM Using a Voltage Vector With Optimal Parameters", *IEEE Transactions on Industrial Electronics*, vol. 63, no. 6, pp. 3876-3888, June 2016.

[15] R. Errouissi, et. al., "Continuous-time model predictive control of a permanent magnet synchronous motor drive with disturbance decoupling", *IET Electric Power Applications*, vol. 11, no. 5, pp. 697-706, 2017.

[16] M. Abdelrahem, C. Hackl, and R. Kennel, "Model Predictive Control of Permanent Magnet Synchronous Generators in Variable-Speed Wind Turbine Systems", *in Proceedings of Power and Energy Student Summit (PESS 2016)*, Aachen, Germany, 19-20 January 2016.

[17] M. Abdelrahem, C. Hackl, R. Kennel, "Simplified Model Predictive Current Control without Mechanical Sensors for Variable-Speed Wind Energy Conversion Systems", *Electrical Engineering Journal*, vol. 99, no. 1, pp. 367-377, 2017.

[18] N. Stati, M. Abdelrahem, M. H. Mobarak, and R. Kennel, "Finite control set-model predictive control with on-line parameter estimation for variable-speed wind energy conversion systems", *IEEE International Symposium on Industrial Electronics (INDEL)*, Banja Luka, pp. 1-6, 2016.

[19] M. Abdelrahem, et. al., "Simple and robust direct-model predictive current control technique for PMSGs in variable-speed wind turbines", *in IEEE International Symposium on Predictive Control of Electrical Drives and Power Electronics (PRECEDE)*, Pilsen, pp. 1-6, 2017.

[20] F. Niu, et. al., "Comparative Evaluation of Direct Torque Control Strategies for Permanent Magnet Synchronous Machines", *IEEE Transactions on Power Electronics*, vol. 31, no. 2, pp. 1408-1424, 2016.

[21] T. Geyer, G. Papafotiou, M. Morari, "Model Predictive Direct Torque Control–Part I: Concept, Algorithm, and Analysis", *IEEE Transactions on Industrial Electronics*, vol. 56, no. 6, pp. 1894-1905, 2009.

[22] P. Cortes and et al., "Guidelines for weighting factors design in Model Predictive Control of power converters and drives", *IEEE International Conference on Industrial Technology*, Gippsland, VIC, pp. 1-7, 2009.

[23] S. A. Davari, D. A. Khaburi, and R. Kennel, "An Improved FCS-MPC Algorithm for an Induction Motor With an Imposed Optimized Weighting Factor", *IEEE Transactions on Power Electronics*, vol. 27, no. 3, pp. 1540-1551, March 2012.

[24] F. Villarroel, et. al. "Multiobjective Switching State Selector for Finite-States Model Predictive Control Based on Fuzzy Decision Making in a Matrix Converter", *IEEE Transactions on Industrial Electronics*, vol. 60, no. 2, pp. 589-599, Feb. 2013.

[25] C. A. Rojas, et. al. "Predictive torque and flux control without weighting factors", *IEEE Trans. Ind. Electron.*, vol. 60, no. 2, pp. 681-690, Feb. 2013.

[26] S. A. Davari, D. A. Khaburi, and R. Kennel, "Using a weighting factor table for FCS-MPC of induction motors with extended prediction horizon", 38^{th} *Annual Conference on IEEE Industrial Electronics Society (IECON)*, Montreal, QC, pp. 2086-2091, 2012.

[27] M. Abdelrahem, et. al., "Predictive Direct Torque Control Strategy for Surface-Mounted Permanent-Magnet Synchronous Generators", *in Conference on sustainable energy supply and energy storage systems (NEIS)*, Hamburg, Germany, pp. 1-6, 2017.

[28] C. Hackl, Non-identifier based adaptive control: Theory and Application, *Springer International Publishing (doi: 10.1007/978-3-319-55036-7)*, 2017.

[29] C. Hackl, et. al., "Current control of reluctance synchronous machines with online adjustment of the controller parameters", *in Proceedings of the 2016 IEEE International Symposium on Industrial Electronics (ISIE 2016)*. Santa Clara, USA, pp. 153-16, 2016.